

## Evidence for a cage effect in the UV photolysis of HBr in Ar-HBr. Theoretical and experimental results

J. Segall<sup>a</sup>, Y. Wen<sup>a</sup>, R. Singer<sup>a</sup>, C. Wittig<sup>a</sup>, A. García-Vela<sup>b,1</sup> and R.B. Gerber<sup>b,c</sup>

<sup>a</sup> Department of Chemistry, University of Southern California, Los Angeles, CA 90089-0482, USA

<sup>b</sup> Department of Physical Chemistry and the Fritz Haber Research Center for Molecular Dynamics, The Hebrew University of Jerusalem, Jerusalem 91904, Israel

<sup>c</sup> Department of Chemistry, University of California at Irvine, Irvine, CA 92717, USA

Received 17 March 1993

Evidence for a cage effect in the 193 nm photodissociation of HBr in the Ar-HBr cluster is found. This effect manifests itself as a tail extending toward lower energies in the hydrogen photofragment kinetic energy distribution (KED). This is a consequence of energy transfer in collisions between the light and the heavy atoms. There is good agreement between the experimental and theoretical KEDs.

There has been considerable interest in recent years in the dynamics of photoinitiated chemical reactions in weakly bound van der Waals (vdW) or hydrogen bonded molecular clusters. One of the more interesting aspects of these systems is the restricted relative geometries of the reactants imposed by the structure of the cluster. Forces between molecules bound together in a cluster may constrain, at least to some extent, their mutual orientations and consequently the angles and impact parameters of a photoinitiated reaction, thereby allowing a higher degree of control over the initial conditions of the reaction than under bulk gas phase conditions [1-8]. The study of chemical reactivity in weakly bound clusters also offers new possibilities for exploring the effect of the weak interactions, or "solvation" bonds, on a reaction. A vdW or hydrogen bonded cluster can be viewed as a "microsolution" in which a molecule is solvated by one or more atoms or molecules. These systems thus provide a useful guide to a better understanding of solvation effects on chemical reactions in condensed matter, with important simplifications due to the relatively small number of degrees of freedom involved in the case of clusters.

The cage effect is one of the most important solvent effects on a reaction. When, for example, an isolated diatomic molecule is electronically excited from its ground state to a repulsive one, the dissociation of the diatomic bond is direct and rapid, with a quantum yield of unity. The behavior of the diatomic molecule can differ greatly from the above picture when it is no longer free, but weakly bound to some solvent atoms or molecules. The surrounding solvent may act as a cage confining the photofragments, and therefore prevent or delay their mutual separation. The occurrence and manifestations of the cage effect in small clusters have been investigated both experimentally [9-12] and theoretically [13,14]. One of these studies explored the dependence of the cage effect on the cluster size for photolysis of HI in the clusters  $Xe_n-HI$  ( $n=1-12$ ) [14], and two of the present authors recently reported calculations on the photolysis of HCl in Ar-HCl [15,16]. These calculations predicted that the presence of even a single Ar atom forms a cage which noticeably delays the departure of a significant fraction of the atomic hydrogen photofragments.

The aim of this Letter is to report and compare experimental and calculated results on the photodissociation of HBr in the Ar-HBr cluster, emphasizing the possible existence of a cage effect. Com-

<sup>1</sup> Permanent address: Instituto de Matemáticas y Física Fundamental, C.S.I.C. C/Serrano 123, 28006 Madrid, Spain.

parison between experiment and theory, not previously available for these systems, is essential to confirm whether, or to what extent, the effect exists. This experimental–theoretical interplay also constitutes a useful test of the accuracy of the potentials and the reliability of the method used to treat the dynamics.

The system studied here involves electronic excitation of the HBr diatomic from its  $^1\Sigma$  ground electronic and  $v=0$  vibrational level at a wavelength of 193 nm, where only the repulsive  $^1\Pi$  and  $^3\Pi$  excited states are energetically accessible. To represent the ground potential surface we use a sum of a pairwise potential for the H–Br interaction plus an anisotropic atom–diatom term for the vdW interaction. The H–Br potential is reproduced by a Morse function with parameters:  $D=31607.456\text{ cm}^{-1}$ ,  $r_{\text{eq}}(\text{HBr})=1.41443\text{ \AA}$  and  $\alpha=1.809\text{ \AA}^{-1}$ . For the vdW term, the H4 potential of Hutson [17] is employed. Such a potential is derived from an analytical fit to molecular-beam microwave and radio frequency spectra of Ar–HBr. As in the case of Ar–HCl, this potential surface predicts a linear equilibrium geometry for Ar–H–Br, with an additional secondary minimum associated with the other linear configuration, namely Ar–Br–H.

The excited-state potentials were taken as sums of atom–atom interactions between the three particles of the system. This is probably the main assumption tested in the comparison of theory with experiment. For the Ar–H interaction term we took the recent Tang and Toennies potential [18]. The Ar–Br potential was modelled as an Ar–Kr interaction for which we used a Morse function fitted to the HFD-C2 potential of Aziz and van Dalen [19], with parameters:  $D=116.2768\text{ cm}^{-1}$ ,  $r_{\text{eq}}(\text{ArBr})=3.881\text{ \AA}$  and  $\alpha=1.6799\text{ \AA}^{-1}$ . Since the Ar–Br interaction does not play a prominent role in the dynamics, replacing it by the Ar–Kr interaction, while a crude approximation, may prove adequate for reconciling the major findings. Finally, for the H–Br interaction in the  $^1\Pi$  and  $^3\Pi$  states, an empirical potential [20] was used – the same for both states. Comparison with experiment also implicitly tests this assumption.

The calculations were done by applying a quasi-classical trajectory approach. Sampling of initial conditions was carried out by using the quantum wavefunction for the zero point vibration of the sys-

tem in the ground electronic state. For each set of positions and momenta sampled, the system is excited vertically to the upper-state surface, in the spirit of a Franck–Condon transition, using an energy corresponding to the 193 nm excitation wavelength employed experimentally. Trajectories describing the photodissociation of the diatomic molecule in the cluster were then integrated on the excited potential.

In previous calculations on HCl photodissociation in Ar–HCl, manifestations of a cage effect were observed in the final angular and kinetic energy distribution (KED) [15,16] of the hydrogen photofragment. The experimental observable corresponding to the KED is the time-of-flight (TOF) spectrum of the hydrogen atom converted to the energy domain. A full description of the present experimental method – high- $n$  Rydberg time-of-flight (HRTOF) spectroscopy of atomic hydrogen – is not possible here; details will be published later. Fig. 1 shows the salient features: (i) expansion cooling of samples using a pulsed nozzle; (ii) excimer laser photodissociation; (iii) Lyman- $\alpha$  excitation of atomic hydrogen with sub-Doppler resolution; (iv) further excitation of the excited hydrogen to optically metastable high- $n$  Rydberg states lying just below the ionization continuum; and (v) detection of the highly excited hydrogen atoms as they pass a mesh 33.6 cm from the focal volume, providing the TOF spectrum.

In addition to the desired binary clusters, there are undoubtedly higher-than-binary clusters (as well as uncomplexed HBr) present in the expansion, and contributions from these species must not be overlooked in scrutinizing the data. When varying the backing pressure and sample composition, the amount of inelastically scattered hydrogen changes smoothly and monotonically, with the smallest

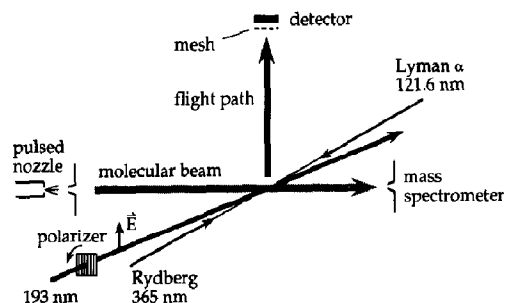


Fig. 1. Schematic drawing of the HRTOF arrangement.

amount of scattering being the most reflective of binary clusters. For the present discussion, we assume that the *majority* of the clusters are binary. However, we cannot completely eliminate the formation of higher complexes in the free jet expansions used here. The experiments detect all hydrogen atoms entering the solid angle subtended by the detector with equal probability, so inevitably the results contain contributions from higher-than-binary clusters. In the future, we will spectroscopically select binary clusters and then photodissociate only these "tagged" species. For the time being, we assume that the presence of higher clusters does not alter our conclusions, which at this stage are qualitative. We shall return to this point later.

Polarized photolysis radiation can be used to align the transition dipoles of dissociating molecules, and for hydrogen halides, parallel and perpendicular transitions are known to display strong halogen atom spin orbit preferences. For 193 nm excitation of HBr, the transition moment is predominantly perpendicular, yielding mainly ground state Br. Because excitation is primarily through a perpendicular transition and photofragmentation is rapid, the spatial distribution of photofragments is anisotropic, even if the photolysis laser is unpolarized, as it is for some of the experimental data presented here (see fig. 2).

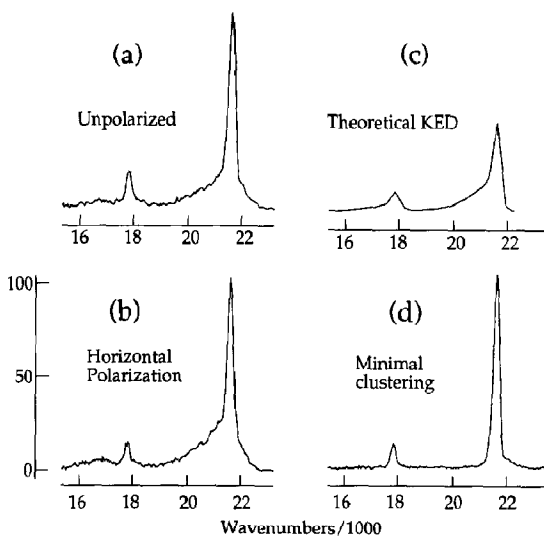


Fig. 2. Translational energy distributions for unpolarized and horizontally polarized photolysis beams. The data contain contributions from uncomplexed HBr; the theoretical curve does not.

Since the scattering process in the Ar-HBr frame is expected to be spatially anisotropic [15,16], and the experiment is sensitive only to hydrogen atoms at a certain laboratory solid angle (see fig. 1), the experiment measures a differential cross section at a fixed laboratory final scattering angle, whereas the calculated KED presented here is integrated over all angles. However, the anisotropy produced by unpolarized photolysis is not large and therefore does not substantially impact the comparison between experiment and calculation. The theoretical KED is presented in fig. 2c for comparison to the main experimental results, i.e. those obtained using unpolarized and horizontally polarized radiations.

Alternatively, the spatial anisotropies can be exploited. For example, hydrogen scattered from the nearby moiety can lead to large signal enhancements, e.g., in cases where the hydrogen atom would not reach the detector *unless* it scatters from the nearby species, as shown in fig. 3. This effect can be seen in fig. 4, which shows hydrogen kinetic energy distributions for cases of significant and minimal clustering. Since photodissociation at 193 nm occurs primarily via a perpendicular transition, signals deriving from uncomplexed material are largest with the photolysis electric field horizontal, i.e. in the plane formed by the molecular and photolysis beams. With the electric field vertical, the signal is relatively small, as shown by the scale change between figs. 2 and 4. However, in fig. 4, one sees that the percentage of the signal that derives from clustered material is much higher than for the case of horizontal polarization shown in fig. 2b. Also, the shapes differ

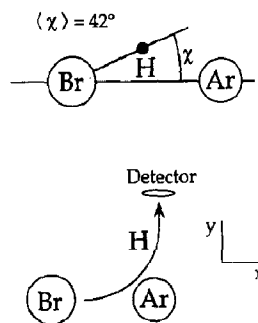


Fig. 3. The Ar-HBr complex is very floppy, so a broad range of angles  $\chi$  is sampled. Vertical polarization (see fig. 1) results in modest signals from uncomplexed HBr. However, "collisions" with the nearby Ar can deflect hydrogen atoms into the detector.

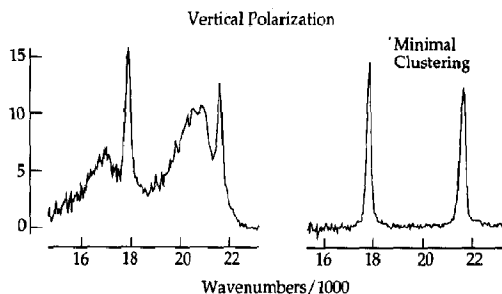


Fig. 4. Left entry (5% HBr in Ar, 225 kPa): with vertical polarization, peaks are present in the translational energy distribution, in contrast to the case of horizontal polarization.

significantly because the KED is a function of the scattering angle. Note that for vertical polarization, the symmetry of the scattered peak intensities confirms that they derive, at least in large part, from the perpendicular transition.

Another important feature seen in fig. 4 is that the energy distribution for the scattered hydrogen atoms peaks  $\approx 1000 \text{ cm}^{-1}$  below the peak for hydrogen atoms that derive from the photolysis of uncomplexed HBr. This can be understood as a consequence of the fact that for this orientation of the photolysis electric field, only strongly scattered hydrogen atoms reach the detector. In fact, the distribution of photoexcited HBr axes peaks in the plane containing the photolysis beam and the molecular beam, and this plane is perpendicular to the line between the interaction region and the detector (see fig. 1). Thus, a hydrogen atom initially moving in this plane must have its trajectory turned by  $\approx 90^\circ$  in order for it to reach the detector, as shown in fig. 3. Solving the classical equations of motion for an initial hydrogen velocity in the  $x$ -direction that is deflected into the  $y$ -direction in a single collision yields:

$$E = E_0 \frac{[M_{\text{Ar}} - M_{\text{H}}]}{[M_{\text{Ar}} + M_{\text{H}}]},$$

where  $E_0 \approx 21600 \text{ cm}^{-1}$  is the hydrogen kinetic energy for 193 nm HBr photolysis. Therefore,  $E_0 - E$  is approximately  $1000 \text{ cm}^{-1}$ , which is in good agreement with the data shown in fig. 4. Were  $\text{Ar}_n\text{-HBr}$  clusters with  $n > 1$  playing a dominant role, this level of agreement would be surprising.

The two peaks in the calculated KED shown in fig. 2c correspond to the two excited  $\Pi$  states of HBr.

The KED corresponding to each  $\Pi$  state was calculated separately, i.e. no coupling between the two excited surfaces was included in the calculations. A statistics of 6000 trajectories was used to describe photodissociation on each surface. By applying the experimental branching ratio between the intensities of the two peaks to the two independently calculated parts of the KED, and adding them together in the energy regions where they overlap, we obtain the calculated distribution. The model could be improved by including coupling between the two excited surfaces and applying a trajectory surface hopping method [21,22].

The most important result of this work is the experimental finding of a cage effect for photolysis of HBr in Ar-HBr. In comparing experimental KEDs for conditions of minimal and significant clustering, we observe that when clusters are present the peaks have tails extending to lower energies. *This is the signature of the cage effect.* As discussed previously (for the case of Ar-HCl [15,16]), the hydrogen is initially trapped between Ar and Br and collides several times with the heavy atoms before leaving the cluster. Consequently, energy transfer occurs from the light to the heavy particles, giving rise to the low energy tails. Even a single atom has a large effect on the dynamics. It is reasonable to anticipate a low energy tail for the Ar-HBr geometry, so observation of this qualitative aspect comes as no surprise. However, the shape of the tail depends on details of the potential. The calculations show that such a tail is the consequence not only of a single collision between the hydrogen atom and the Ar "solvent", but involves also contributions from "rattling" vibrations of the hydrogen between the heavy atoms, i.e. multiple collisional events. We find that events with up to five such collisions make contributions. This is in accord with previous findings for Ar-HCl [14]. It also confirms the "squeezed atom effect" (or the cage effect) that has been proposed for photoinitiated reactions in weakly bonded clusters such as  $\text{CO}_2\text{-HX}$  [23].

The agreement between the experimental and calculated KEDs shows that classical mechanics can describe the dynamics of systems involving heavy and fast, light atoms. It also supports the approximation made for the excited state potentials, i.e. using the same curve for the two  $\Pi$  states. The underlying assumption is that at the energies involved, the slopes

of both potential curves, which ultimately determine the dissociation dynamics, are similar. Perhaps most important, the theory-experiment agreement indicates that the pairwise atom-atom potentials used for the excited state describe adequately the solvent-reagent interaction in these systems. This suggests that it should be justified to use such potentials for corresponding condensed matter systems, e.g. photolysis of HBr in solid or liquid Ar.

Finally, the agreement between the calculations and the experiments supports the contention that a major role for higher clusters in this case seems unlikely. We note that calculations for  $\text{Xe}_n\text{-HI}$  clusters have shown a dramatic change in the kinetic energy distribution of hydrogen atoms for clusters with  $n \geq 5$  [14]. If larger clusters had been present to a major extent, such an agreement would not have been possible.

Discrepancies remain, e.g., in the asymptotic regions of the tails and the high-energy sides of the peaks. These are believed to be due mainly to: (i) experimental aspects such as contributions from higher clusters; and (ii) theoretical considerations such as the potential surface and the classical model, e.g. the deviation of the excited state potential used from the true one is probably a source of error. We note that disagreement in the low-energy asymptotic region of the tails corresponds to many-collision events that have low probability. To describe more accurately those regions of the KED, a more refined theoretical model and potential surfaces should be used. At the level of the present work our main theoretical goals are achieved by reproducing most of the experimental KED.

In addition to the observation of slower hydrogen deriving from clusters, there is an unmistakable contribution at kinetic energies that are higher than for unclustered material. We note that such "blue-shifts" can be due to: (i) the fact that hydrogen receives a larger share of the center-of-mass translational energy when the Ar-Br species remains compared to when just Br remains; (ii) velocity slip of the heavy species relative to the lighter carrier; and (iii) the Ar-Br photoproduct being more strongly bound than Ar-HBr. A large percentage of the photodissociation events clearly result in the Ar-Br diatom being formed. Moreover, the photolytic stripping of atomic hydrogen can be a general means of preparing rad-

ical-molecule complexes, which are desirable for spectroscopic and reactive scattering experiments. For example, it may be possible to spectroscopically examine interactions of excited  $2P_{1/2}$  halogens with nearby species.

Experiments such as those reported herein can help elucidate the equilibrium geometry and even vibrational wavefunctions in clusters of this type, albeit qualitatively. For example, a hydrogen KED with a low-energy tail is the signature of collisions, as a consequence of a cluster geometry in which the hydrogen lies mainly between the Ar and Br atoms. On the other hand, an equilibrium geometry like Ar-Br-H would yield a hydrogen KED similar to that shown in fig. 2d, since direct hydrogen departure is favored by this geometry. Something close to this is observed when HI/Ar mixtures are expanded (5%, 100-400 kPa). We find that there is no low-energy tail whatsoever. On the contrary, there is a modest but conspicuous blue-shift. This stands in stark contrast to HBr/Ar expansions, where the low-energy tail is the dominant signature. We interpret this as evidence for the H-I-Ar structure in which the hydrogen points away from the Ar, allowing it to leave without scattering from Ar. Inevitably, I-Ar remains.

To conclude, we have found, both experimentally and theoretically, signatures of a cage effect in the photolysis of HBr in Ar-HBr, due to the presence of the Ar atom. This effect manifests itself in tails of the hydrogen photofragment KED toward the low-energy side, as a consequence of energy transfer due to multiple collisions between the light and the heavy particles. This confirms predictions of this effect in a similar cluster (Ar-HCl) and evidences the large influence of even a single solvent atom on the photodissociation process. The modest discrepancies between experiment and theory are probably due to the excited-state potentials used and the classical treatment, as well as our inability to eliminate experimental contributions from higher-than-binary clusters. The results suggest that pairwise atom-atom potentials can be used to describe the reagent-solvent interaction in the excited state of such clusters, and probably of related condensed matter systems as well.

We thank Professor J.A. Beswick for helpful comments. The Fritz Haber Research Center is sup-

ported by the Minerva Gesellschaft für die Forschung, mbH, Munich, Germany. The work at USC was supported by the US Department of Energy (DE-FG03-85ER13363).

## References

- [1] C. Jouvét and B. Soep, *Chem. Phys. Letters* 96 (1983) 426.
- [2] W.H. Breckenridge, C. Jouvét and B. Soep, *J. Chem. Phys.* 84 (1986) 1443;  
C. Jouvét, M. Boivineau, M.C. Duval and B. Soep, *J. Phys. Chem.* 91 (1987) 5416.
- [3] M. Boivineau, J.L. Calve, M.C. Castex and C. Jouvét, *Chem. Phys. Letters* 130 (1986) 208.
- [4] S. Buelow, G. Radhakrishnan, J. Catanzarite and C. Wittig, *J. Chem. Phys.* 83 (1985) 444;  
S. Buelow, M. Noble, G. Radhakrishnan, H. Reisler, C. Wittig and G. Hancock, *J. Phys. Chem.* 90 (1986) 1015.
- [5] C. Wittig, S. Sharpe and R.A. Beaudet, *Accounts Chem. Res.* 21 (1988) 341.
- [6] C. Wittig, Y.M. Engel and R.D. Levine, *Chem. Phys. Letters* 153 (1988) 411.
- [7] E. Böhmer, S.K. Shin, Y. Chen and C. Wittig, *J. Chem. Phys.* 97 (1992) 2536.
- [8] N.F. Scherer, L.R. Khundkar, R.B. Bernstein and A.H. Zewail, *J. Chem. Phys.* 87 (1987) 1451;  
N.F. Scherer, C. Sipes, R.B. Bernstein and A.H. Zewail, *J. Chem. Phys.* 92 (1990) 5239.
- [9] J.J. Valentini and J.B. Cross, *J. Chem. Phys.* 77 (1982) 572.
- [10] J.M. Philipoz, P. Melinon, R. Monot and H. van den Bergh, *Chem. Phys. Letters* 138 (1987) 579.
- [11] J.M. Philipoz, H. van den Bergh and R. Monot, *J. Phys. Chem.* 91 (1987) 2545.
- [12] J.M. Philipoz, R. Monot and H. van den Bergh, *J. Chem. Phys.* 93 (1990) 8676.
- [13] J.A. Beswick, R. Monot, J.M. Philipoz and H. van den Bergh, *J. Chem. Phys.* 86 (1987) 3965.
- [14] R. Alimi and R.B. Gerber, *Phys. Rev. Letters* 64 (1990) 1453.
- [15] A. García-Vela, R.B. Gerber and J.J. Valentini, *Chem. Phys. Letters* 186 (1991) 223.
- [16] A. García-Vela, R.B. Gerber and J.J. Valentini, *J. Chem. Phys.* 97 (1992) 3297.
- [17] J.M. Hutson, *J. Chem. Phys.* 91 (1989) 4455.
- [18] K.T. Tang and J.P. Toennies, *Chem. Phys.* 156 (1991) 413.
- [19] R.A. Aziz and A. van Dalen, *J. Chem. Phys.* 78 (1983) 2413.
- [20] C.F. Goodeve and A.W.C. Taylor, *Proc. Roy. Soc. A* 152 (1935) 221.
- [21] J.C. Tully and R.K. Preston, *J. Chem. Phys.* 55 (1971) 562;  
J.C. Tully, in: *Dynamics of molecular collisions, Part B*, ed. W.H. Miller (Plenum Press, New York, 1976) p. 217.
- [22] S. Miret-Artés, G. Delgado-Barrio, O. Atabek and R. Lefebvre, *N. J. Chim.* 6 (1982) 431.
- [23] C. Wittig, Y.M. Engel and R.D. Levine, *Chem. Phys. Letters* 153 (1988) 411.